molecular pharmaceutics

Article

Cite This: *Mol. Pharmaceutics* 2018, 15, 5183−5191

pubs.acs.org/molecularpharmaceutics

Enhancing Treatment Efficacy of ^{177}Lu-PSMA-617 with the Conjugation of an Albumin-Binding Motif: Preclinical Dosimetry and Endoradiotherapy Studies

Hsiou-Ting Kuo,[†] Helen Merkens,[†] Zhengxing Zhang,[†] Carlos F. Uribe,[†] Joseph Lau,[†] Chengcheng Zhang,[†] Nadine Colpo,[†] Kuo-Shyan Lin,*[,†,‡,§] and François Bénard*[,†,‡,§]

[†]Department of Molecular Oncology, BC Cancer, Vancouver, BC V5Z 1L3, Canada

[‡]Department of Functional Imaging, BC Cancer, Vancouver, BC V5Z 4E6, Canada

[§]Department of Radiology, University of British Columbia, Vancouver, BC V5Z 1M9, Canada

Supporting Information

ABSTRACT: We designed and evaluated a novel albumin-binder-conjugated ^{177}Lu-PSMA-617 derivative, ^{177}Lu-HTK01169, with an extended blood retention time to maximize the radiation dose delivered to prostate tumors expressing prostate-specific membrane antigen (PSMA). PSMA-617 and HTK01169 that contained *N*-[4-(*p*-iodophenyl)butanoyl]-Glu as an albumin-binding motif were synthesized using the solid-phase approach. Binding affinity to PSMA was determined by in vitro competition-binding assay. ^{177}Lu labeling was performed in acetate buffer (pH 4.5) at 90 °C for 15 min. SPECT/CT imaging, biodistribution, and endoradiotherapy studies were conducted in mice bearing PSMA-expressing LNCaP tumor xenografts. Radiation dosimetry was calculated using OLINDA software. Lu-PSMA-617 and Lu-HTK01169-bound PSMA with high affinity (K_i values = 0.24 and 0.04 nM, respectively). SPECT imaging and biodistribution studies showed that ^{177}Lu-PSMA-617 and ^{177}Lu-HTK01169 were excreted mainly via the renal pathway. With fast blood clearance (0.68%ID/g at 1 h postinjection), the tumor uptake of ^{177}Lu-PSMA-617 peaked at 1 h postinjection (15.1%ID/g) and gradually decreased to 7.91%ID/g at 120 h postinjection. With extended blood retention (16.6 and 2.10%ID/g at 1 and 24 h, respectively), the tumor uptake of ^{177}Lu-HTK01169 peaked at 24 h postinjection (55.9%ID/g) and remained at the same level by the end of the study (120 h). Based on dosimetry calculations, ^{177}Lu-HTK01169 delivered an 8.3-fold higher radiation dose than ^{177}Lu-PSMA-617 to LNCaP tumor xenografts. For the endoradiotherapy study, the mice treated with ^{177}Lu-PSMA-617 (18.5 MBq) all reached humane end point (tumor volume >1000 mm^3) by Day 73 with a median survival of 58 days. Mice treated with 18.5, 9.3, 4.6, or 2.3 MBq of ^{177}Lu-HTK01169 had a median survival of >120, 103, 61, and 28 days, respectively. With greatly enhanced tumor uptake and treatment efficacy compared to ^{177}Lu-PSMA-617 in preclinical studies, ^{177}Lu-HTK01169 warrants further investigation for endoradiotherapy of prostate cancer.

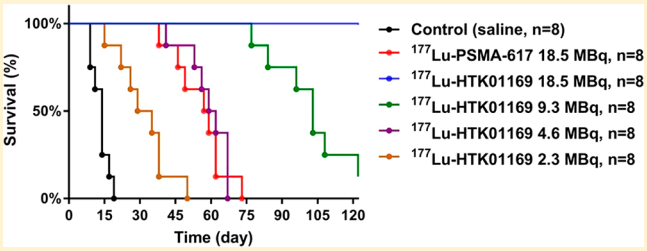

KEYWORDS: *prostate-specific membrane antigen, lutetium-177, albumin binder, PSMA-617, endoradiotherapy*

INTRODUCTION

Prostate-specific membrane antigen (PSMA) is a transmembrane protein that catalyzes the hydrolysis of *N*-acetylaspartylglutamate to glutamate and *N*-acetylaspartate.[1] PSMA is not expressed in most normal tissues but is overexpressed (up to 1000-fold) in prostate tumors and metastases.[2,3] Due to its pathological expression pattern, various radiolabeled PSMA-targeting constructs have been designed and evaluated for endoradiotherapy of prostate cancer.[4−7]

The common radiotherapeutic isotopes used for the design of PSMA-targeting agents include ^{131}I (β-emitter, $t_{1/2}$ = 8.03 d), ^{90}Y (β-emitter, $t_{1/2}$ = 2.66 d), ^{177}Lu (β-emitter, $t_{1/2}$ = 6.65 d) and ^{225}Ac (α-emitter, $t_{1/2}$ = 9.95 d). As a halogen, ^{131}I is normally incorporated into the PSMA-targeting agents via an electrophilic substitution reaction, whereas as metals, ^{90}Y, ^{177}Lu, and ^{225}Ac are often complexed by a polyaminocarboxylate chelator such as DOTA (1,4,7,10-tetraazacyclododecane-1,4,7,10-tetraacetic acid).

The common radiolabeled PSMA-targeting endoradiotherapeutic agents are derivatives of lysine−urea−glutamate (Lys−urea−Glu) including ^{131}I-MIP-1095, ^{177}Lu-PSMA-617, and ^{177}Lu-PSMA I&T (Figure 1).[5−7] Among them, ^{177}Lu-PSMA-617 is the most studied agent and is currently being evaluated in multicenter trials.[7−14] Preliminary data demonstrated that ^{177}Lu-PSMA-617 was effective in treating metastatic prostate

Received: July 10, 2018
Revised: September 10, 2018
Accepted: September 25, 2018
Published: September 25, 2018

DOI: 10.1021/acs.molpharmaceut.8b00720
Mol. Pharmaceutics 2018, 15, 5183−5191

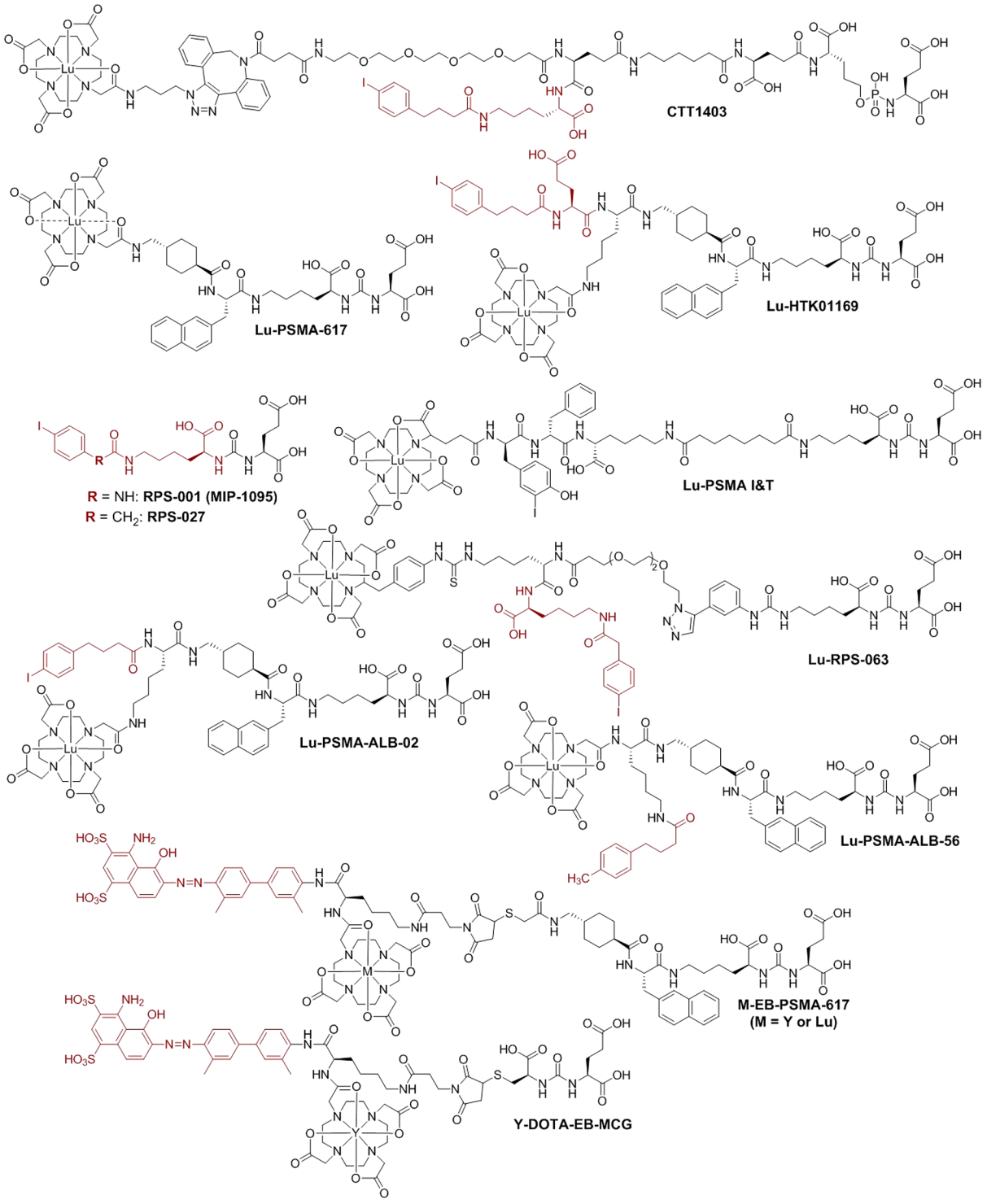

Figure 1. Chemical structures of reported PSMA-targeted endoradiotherapeutic agents. Several of the compounds have incorporated an albumin binder motif, shown in brown.

cancer with 32−60% of patients having >50% reduction in PSA levels and without severe side effects.[7−13] In a phase 2 Australian study, an objective response was observed in 82% of patients with measurable nodal or visceral disease.[14] However, the complete response rate was low (<7%), and up to 33% of the patients still had progressive disease after ^{177}Lu-PSMA-617 treatment.[7,9−13] Interestingly, a recent report showed impressive responses with ^{225}Ac-PSMA-617 (replacing ^{177}Lu with an α-emitter ^{225}Ac) in advanced metastatic prostate cancer patients, including one subject whose disease had progressed despite ^{177}Lu-PSMA-617 therapy.[15]

Despite the great potential of ^{225}Ac-PSMA-617 for endoradiotherapy, the supply of ^{225}Ac is globally limited. More effective ^{177}Lu-labeled PSMA-targeting agents will have a greater immediate impact for endoradiotherapy of prostate cancer than ^{225}Ac-PSMA-617, as good manufacturing practice (GMP) compliant ^{177}Lu is commercially available in larger quantities from multiple suppliers. The greater efficacy of ^{225}Ac-PSMA-617

DOI: 10.1021/acs.molpharmaceut.8b00720
Mol. Pharmaceutics 2018, 15, 5183−5191

may be due to the high linear energy transfer of α-particles, which causes double strand breaks that may be less susceptible to radiation resistance compared to the indirect damage produced by β-particles emitted by ^{177}Lu. One approach to increase the radiotherapeutic efficacy is to increase the radiation dose deposited in tumors per unit of administered radioactivity of the ^{177}Lu-labeled agents. Improving the delivery of ^{177}Lu to tumors can also reduce the cost of therapeutic radiopharmaceuticals by decreasing radioisotope costs.

In this study, we designed and synthesized ^{177}Lu-HTK01169 (Figure 1), a close analogue of ^{177}Lu-PSMA-617 conjugated with a novel albumin-binding motif *N*-[4-(*p*-iodophenyl)-butanoyl]-Glu to extend its blood retention time and maximize uptake in PSMA-expressing prostate tumors. Head-to-head comparisons between ^{177}Lu-HTK01169 and ^{177}Lu-PSMA-617 were conducted by in vitro competition-binding and plasma-protein-binding assays, as well as by SEPCT/CT imaging, biodistribution, and endoradiotherapy studies in mice bearing PSMA-expressing LNCaP tumor xenografts.

MATERIALS AND METHODS

General Methods. All chemicals and solvents were obtained from commercial sources and used without further purification. Human serum for the protein-binding assay was obtained from Innovative Research (Novi, MI). PSMA-617 and HTK01169 were synthesized using a solid-phase approach on an Aapptec (Louisville, KY) Endeavor 90 peptide synthesizer. Mass analyses were performed using an AB SCIEX (Framingham, MA) 4000 QTRAP mass spectrometer system with an ESI ion source. Purification and quality control of nonradioactive and ^{177}Lu-labeled peptides were performed on Agilent (Santa Clara, CA) HPLC systems equipped with a model 1200 quaternary pump and a model 1200 UV absorbance detector. The radio-HPLC system was equipped with a Bioscan (Washington, DC) NaI scintillation detector. The HPLC columns used were a Phenomenex (Torrance, CA) semipreparative column (Luna C18, 5 μm, 250 × 10 mm) and a Phenomenex analytical column (Luna C18, 5 μm, 250 × 4.6 mm). Radioactivity of ^{177}Lu-labeled peptides was measured using a Capintec (Ramsey, NJ) CRC-25R/W dose calibrator.

Solid-Phase Synthesis of PSMA-617 and HTK01169. Synthesis of PSMA-617 and its albumin-binder-containing derivative HTK01169 was modified from reported procedures,[16] starting from Fmoc−Lys(ivDde)−Wang resin. After the isocyanate of the *t*-butyl-protected glutamyl moiety was coupled,[17] the ivDde-protecting group was removed with 2% hydrazine in *N*,*N*-dimethylformamide (DMF). Subsequent coupling of Fmoc−2-Nal−OH, Fmoc−tranexamic acid, and DOTA-tris(*t*-bu)ester, followed by trifluoroacetic acid (TFA) cleavage, provided the crude product of PSMA-617. After HPLC purification using the semipreparative column with 25% acetonitrile in water containing 0.1% TFA at a flow rate of 4.5 mL/min (t_R = 10.5 min), PSMA-617 was obtained in 25% yield. ESI-MS: calculated $[M + H]^+$ for PSMA-617 $C_{49}H_{72}N_9O_{16}$ 1042.5; found $[M + H]^+$ 1042.6.

For the synthesis of HTK01169, Fmoc−Lys(ivDde)−OH was coupled to the sequence after Fmoc−tranexamic acid. Elongation was continued with the addition of Fmoc−Glu(tBu)−OH and 4-(*p*-iodophenyl)butyric acid to the *N*-terminus. Subsequently, the ivDde-protecting group was removed with 2% hydrazine in DMF, and DOTA-tris(*t*-bu)ester was coupled to the Lys side chain. The peptide was cleaved with TFA treatment and purified by HPLC using the semipreparative column with 37% acetonitrile in water containing 0.1% TFA at a flow rate of 4.5 mL/min (t_R = 9.7 min). The yield of HTK01169 was 21%. ESI-MS: calculated $[M + H]^+$ for HTK01169 $C_{70}H_{100}N_{12}O_{21}I$ 1571.6; found $[M + H]^+$ 1571.7.

Synthesis of Lu-PSMA-617 and Lu-HTK01169. A solution of PSMA-617 (5.5 mg, 5.3 μmol) or HTK01169 (4.1 mg, 2.6 μmol) was incubated with $LuCl_3$ (5 equiv) in NaOAc buffer (0.1 M, 500 μL, pH 4.2) at 90 °C for 15 min and then purified by HPLC using the semipreparative column. For Lu-PSMA-617, the HPLC conditions were 25% acetonitrile in water with 0.1% TFA at a flow rate of 4.5 mL/min (t_R = 9.7 min). The yield was 62%. ESI-MS: calculated $[M + H]^+$ for Lu-PSMA-617 $C_{49}H_{69}N_9O_{16}$[Lu] 1214.4; found $[M + H]^+$ 1214.4. For Lu-HTK01169, the HPLC conditions were 37% acetonitrile in water with 0.1% TFA at a flow rate of 4.5 mL/min (t_R = 10.0 min). The yield was 31%. ESI-MS: calculated $[M + H]^+$ for Lu-HTK01169 $C_{70}H_{97}N_{12}O_{21}I$[Lu] 1743.5; found $[M + H]^+$ 1743.9.

In Vitro Competition-Binding Assay. In vitro competition-binding assays were conducted as previously reported using LNCaP prostate cancer cells and ^{18}F-DCFPyL as the radioligand.[18] Briefly, LNCaP cells (400 000/well) were plated onto a 24-well poly-D-lysine coated plate for 48 h. Growth media was removed and replaced with HEPES buffered saline (50 mM HEPES, pH 7.5, 0.9% sodium chloride), and the cells were incubated for 1 h at 37 °C. ^{18}F-DCFPyL (0.1 nM) was added to each well (in triplicate) containing various concentrations (0.5 mM−0.05 nM) of tested compounds (Lu-PSMA-617 or Lu-HTK01169). Nonspecific binding was determined in the presence of 10 μM nonradiolabeled DCFPyL. The assay mixtures were further incubated for 1 h at 37 °C with gentle agitation. Then, the buffer and hot ligand were removed, and cells were washed twice with cold HEPES buffered saline. To harvest the cells, 400 μL of 0.25% trypsin solution was added to each well. Radioactivity was measured on a PerkinElmer (Waltham, MA) Wizard2 2480 automatic gamma counter. Nonlinear regression analyses and K_i calculations were performed using the GraphPad Prism 7 software.

Synthesis of ^{177}Lu-PSMA-617 and ^{177}Lu-HTK01169. $^{177}LuCl_3$ (329.3−769.9 MBq in 10−20 μL) was added to a solution of PSMA-617 or HTK01169 (25 μg) in NaOAc buffer (0.5 mL, 0.1 M, pH 4.5). The mixture was incubated at 90 °C for 15 min and then purified by HPLC. The HPLC purification conditions (semiprep column, 4.5 mL/min) for ^{177}Lu-PSMA-617 and ^{177}Lu-HTK01169 were 23 and 36% acetonitrile in water (0.1% TFA), respectively. The retention times for ^{177}Lu-PSMA-617 and ^{177}Lu-HTK01169 were 15.0 and 13.8 min, respectively. Quality control was performed on the analytical column with a flow rate of 2 mL/min using the corresponding purification solvent conditions. The retention times for ^{177}Lu-PSMA-617 and ^{177}Lu-HTK01169 were both around 5.5 min.

Plasma-Protein-Binding Assay. Plasma-protein-binding assays were performed according to literature methods.[19] Briefly, 37 kBq of ^{177}Lu-PSMA-617 or ^{177}Lu-HTK01169 in 50 μL of PBS was added into 200 μL of human serum, and the mixture was incubated at room temperature for 1 min. The mixture was then loaded onto a membrane filter (Nanosep, 30 K, Pall Corporation, USA) and centrifuged for 45 min (30 130*g*). Saline (50 μL) was added, and centrifugation was continued for another 15 min. The top part with the membrane filter and the bottom part with the solution were counted on a gamma counter. For control, saline was used in place of human serum.

DOI: 10.1021/acs.molpharmaceut.8b00720
Mol. Pharmaceutics 2018, 15, 5183−5191

SPECT/CT Imaging, Biodistribution, and Endoradiotherapy Studies. SPECT/CT imaging and biodistribution were performed using NOD-*scid* IL2Rgamma^{null} (NSG) male mice, and the endoradiotherapy study was conducted using NOD.Cg-Rag1^{tm1Mom} Il2rg^{tm1Wjl}/SzJ (NRG) male mice. The mice were maintained, and the experiments were conducted according to the guidelines established by the Canadian Council on Animal Care and approved by the Animal Ethics Committee of the University of British Columbia. Mice were anesthetized by inhalation with 2% isoflurane in oxygen and implanted subcutaneously with 1×10^7 LNCaP cells posterior to the left shoulder. Mice were used for studies when the tumor reached 5−8 mm in diameter 5−6 weeks after inoculation.

SPECT/CT imaging experiments were conducted using the MILabs (Utrecht, The Netherlands) U-SPECT-II/CT scanner. Each tumor-bearing mouse was injected with ∼37 MBq of ^{177}Lu-labeled PSMA-617 or HTK01169 through the tail vein under anesthesia (2% isoflurane in oxygen). The mice were allowed to recover and roam freely in their cage and imaged at 4, 24, 72, and 120 h after injection. At each time point, the mice were sedated again and positioned in the scanner. A 5 min CT scan was conducted first for anatomical reference with a voltage setting at 60 kV and current at 615 μA followed by a 60 min static emission scan acquired in list mode using an ultrahigh-resolution multipinhole rat-mouse (1 mm pinhole size) collimator. Data were reconstructed using the U-SPECT II software with a 20% window width on three energy windows. The photopeak window was centered at 208 keV, with lower scatter and upper scatter windows centered at 170 and 255 keV, respectively. The images were reconstructed using the ordered subset expectation maximization algorithm (3 iterations, 16 subsets) and a 0.5 mm postprocessing Gaussian filter. Images were decay corrected to injection time in PMOD (PMOD Technologies, Switzerland) and then converted to DICOM for qualitative visualization in the Inveon Research Workplace software (Siemens Medical Solutions USA, Inc.).

For biodistribution studies, the mice were injected with ^{177}Lu-labeled PSMA-617 or HTK01169 (2−4 MBq) as described above. At predetermined time points (1, 4, 24, 72, or 120 h postinjection), the mice were euthanized by CO_2 inhalation. Blood was withdrawn immediately from the heart, and the organs/tissues of interest were collected. The collected organs/tissues were weighed and counted using an automated gamma counter. For the blocking study, mice were coinjected with ^{177}Lu-HTK01169 (2−4 MBq) and 50 nmol of the nonradioactive standard, and organs/tissues of interest were collected at 4 h postinjection.

For radiotherapy study, tumor-bearing mice were injected with saline (the control group), ^{177}Lu-PSMA-617 (18.5 MBq), or ^{177}Lu-HTK01169 (18.5, 9.3, 4.6, or 2.3 MBq) (n = 8 per group). Tumor size and body weight were measured twice a week from the date of injection (Day 0) until completion of the study (Day 120). End point criteria were defined as >20% weight loss, tumor volume >1000 mm^3, or active ulceration of the tumor.

Radiation Dosimetry Calculations. These methods are provided in the Supporting Information.

RESULTS

Peptide Synthesis and Radiochemistry. PSMA-617 and HTK01169 were synthesized in 25 and 21% yields, respectively. After reacting with $LuCl_3$ followed by HPLC purification, Lu-PSMA-617 and Lu-HTK01169 were obtained in 62 and 31% yields, respectively. The identities of PSMA-617, HTK01169, and their Lu complexes were confirmed by MS analyses.

^{177}Lu labeling was conducted in acetate buffer (pH 4.5) at 90 °C followed by HPLC purification. ^{177}Lu-PSMA-617 was obtained in 86.0 ± 1.7% (n = 3) radiochemical yield with 782 ± 43.3 GBq/μmol molar activity and >99% radiochemical purity. ^{177}Lu-HTK01169 was obtained in 63.0 ± 16.2% (n = 4) radiochemical yield with 170 ± 73.6 GBq/μmol molar activity and >99% radiochemical purity. The HPLC chromatograms for semipreparative purification and quality control to confirm identities of ^{177}Lu-PSMA-617 and ^{177}Lu-HTK01169 are provided as Supplemental Figures 1−4.

Binding to PSMA and Serum Proteins. Lu-PSMA-617 and Lu-HTK01169 inhibited the binding of ^{18}F-DCFPyL to PSMA on LNCaP cells in a dose dependent manner (Figure 2),

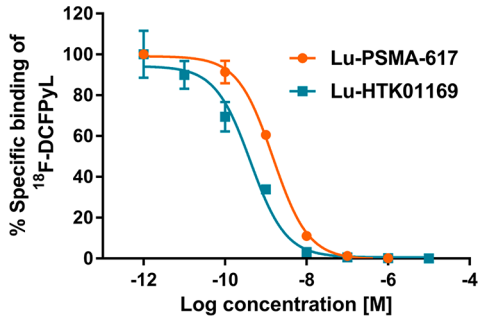

Figure 2. Representative displacement curves of ^{18}F-DCFPyL by Lu-PSMA-617 and Lu-HTK01169. The assays were performed in triplicate.

and their calculated K_i values were 0.24 ± 0.06 and 0.04 ± 0.01 nM (n = 3), respectively. After incubation with saline and centrifugation, the filter-bound radioactivities were 5.21 ± 1.42 and 25.8 ± 3.42% (n = 3) for ^{177}Lu-PSMA-617 and ^{177}Lu-HTK01169, respectively. Replacing saline with human serum increased the filter-bound radioactivities to 82.7 ± 0.32 and 99.2 ± 0.02% (n = 3) for ^{177}Lu-PSMA-617 and ^{177}Lu-HTK01169, respectively, under the same conditions.

SPECT/CT Imaging and Biodistribution. SPECT/CT imaging studies showed that both ^{177}Lu-PSMA-617 and ^{177}Lu-HTK01169 were excreted mainly via the renal pathway with higher renal retention of ^{177}Lu-HTK01169 especially at early time points (4 and 24 h, Figure 3). Higher and sustained tumor uptake was observed for ^{177}Lu-HTK01169. The biodistribution data of ^{177}Lu-PSMA-617 and ^{177}Lu-HTK01169 are

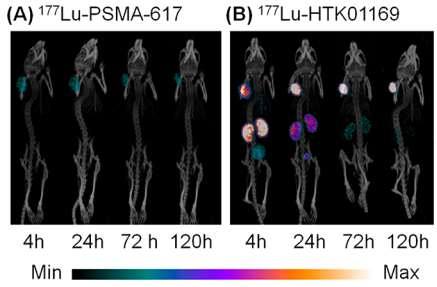

Figure 3. SPECT/CT images of ^{177}Lu-labeled PSMA-617 and HTK01169 in mice bearing LNCaP xenografts.

DOI: 10.1021/acs.molpharmaceut.8b00720
Mol. Pharmaceutics 2018, 15, 5183−5191

shown in Figure 4 (also Supplemental Tables 1 and 2). These data were consistent with the observations from SPECT/CT images.

^{177}Lu-PSMA-617 cleared rapidly from blood and nontarget organs/tissues. At 1 h postinjection, there was only 0.68 ± 0.23%ID/g left in blood. Uptake was observed in PSMA-expressing tissues including spleen (3.34 ± 1.77%ID/g), adrenal glands (4.88 ± 2.41%ID/g), kidneys (97.2 ± 19.4% ID/g), lung (1.34 ± 0.39%ID/g), and LNCaP tumors (15.1 ± 5.58%ID/g).[20,21] The tumor uptake decreased gradually to 7.91 ± 2.82%ID/g at 120 h postinjection. Due to faster clearance from other tissues/organs, the tumor-to-background contrast ratios of ^{177}Lu-PSMA-617 improved over time (Supplemental Table 1).

With a built-in albumin binder, the blood clearance of ^{177}Lu-HTK01169 was relatively slower than that of ^{177}Lu-PSMA-617 (Figure 4). The tumor uptake of ^{177}Lu-HTK01169 increased

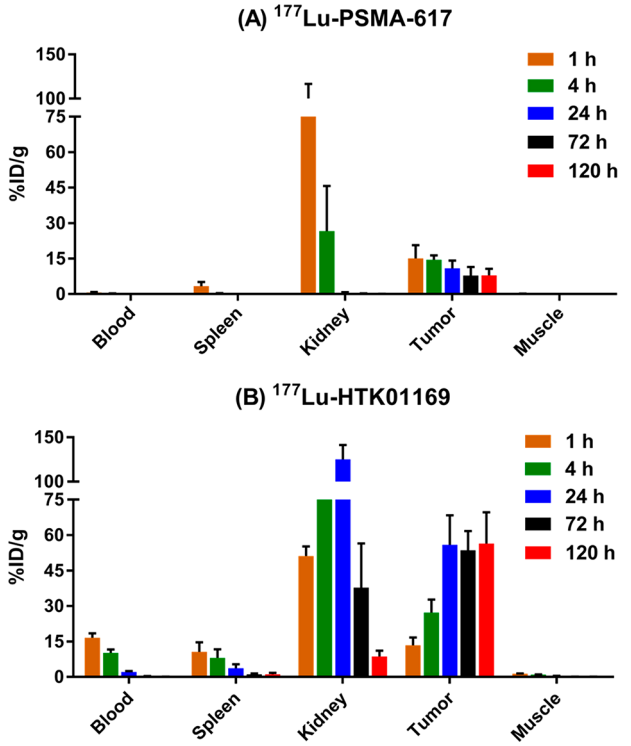

Figure 4. Biodistribution of (A) ^{177}Lu-PSMA-617 and (B) ^{177}Lu-HTK01169 for selected organs in mice bearing LNCaP tumor xenografts ($n \geq 5$).

continuously at early time points, peaked at 24 h postinjection (55.9 ± 12.5%ID/g), and was sustained over the course of the study (56.4 ± 13.2%ID/g at 120 h). Similar to ^{177}Lu-PSMA-617, uptake was also observed in the spleen, adrenal glands, kidneys, and lung (Supplemental Table 2). The tumor-to-background contrast ratios of ^{177}Lu-PSMA-617 improved over time as well, due to sustained uptake in tumor and relatively faster clearance from other organs/tissues. Compared with the biodistribution data collected at the same time point (4 h), blocking with the cold standard reduced uptake in all collected tissues/organs, especially the PSMA-expressing kidneys (125 ± 16.4 vs 5.50 ± 1.95%ID/g) and LNCaP tumors (55.9 ± 12.5 vs 1.70 ± 0.28% ID/g).

Radiation Dosimetry Calculations. Based on the biodistribution data obtained from tumor-bearing mice, an estimate of radiation doses delivered to major organs/tissues of mice was calculated using the OLINDA software. The results are shown in Figure 5 and Supplemental Table 3, where both the

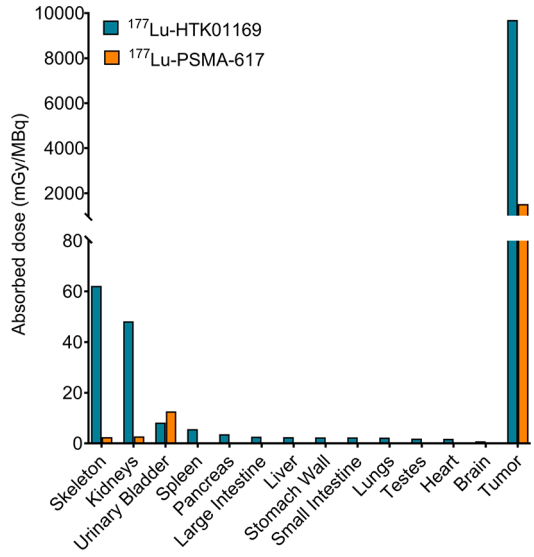

Figure 5. Radiation doses (mGy/MBq) delivered by ^{177}Lu-PSMA-617 and ^{177}Lu-HTK01169 to major organs/tissues of a 25 g mouse calculated using the OLINDA software.

input kinetics of the source organs calculated from the data fit (MBq·h/MBq) and the doses to the target organs (mGy/MBq) are presented. Compared to ^{177}Lu-PSMA-617, ^{177}Lu-HTK01169 delivered 9.4- to 23.1-fold higher radiation doses to all major organs except the urinary bladder, which received a 1.5-fold higher radiation dose from ^{177}Lu-PSMA-617.

Similar results were obtained for calculated radiation doses delivered to human organs/tissues (Supplemental Table 4). Most human organs/tissues would receive 11.9- to 24.9-fold higher radiation doses from ^{177}Lu-HTK01169. Notably, the brain, heart, red marrow, and spleen would receive 6.0-, 50.4-, 30.4-, and 28.1-fold higher doses with ^{77}Lu-HTK01169. The urinary bladder would receive a 1.3-fold higher radiation dose from ^{177}Lu-PSMA-617.

The behavior of radiation doses delivered to unit density spheres based on the kinetics of LNCaP tumors from ^{177}Lu-PSMA-617 and ^{177}Lu-HTK01169 are shown in Figure 6 and Supplemental Table 5. The kinetic uptake values used as input in OLINDA were 3.80 and 31.72 MBq·h/MBq for ^{177}Lu-PSMA-617 and ^{177}Lu-HTK01169, respectively. ^{177}Lu-HTK01169 delivered an 8.3-fold higher radiation dose to LNCaP tumors than ^{177}Lu-PSMA-617 regardless of simulated sphere (tumor) sizes.

Endoradiotherapy Studies. The results of the endoradiotherapy study are shown in Table 1 and Figure 7, and the changes of LNCaP tumor volume and mouse body weight over time after treatment are shown in Figures S5−S10. The tumor volume of the control group (Group A in Table 1 and Figure S5) increased continuously after treatment (saline injection), and the median survival of the control group was only 14 days (mice were euthanized when their tumor volume reached 1000 mm^3). The tumors in mice treated with ^{177}Lu-PSMA-617 (18.5 MBq, Group B in Table 1 and Figure S6) shrank initially but grew back later, leading to an improved median survival of 58 days. The changes in tumor size over time for the mice

DOI: 10.1021/acs.molpharmaceut.8b00720
Mol. Pharmaceutics 2018, 15, 5183−5191

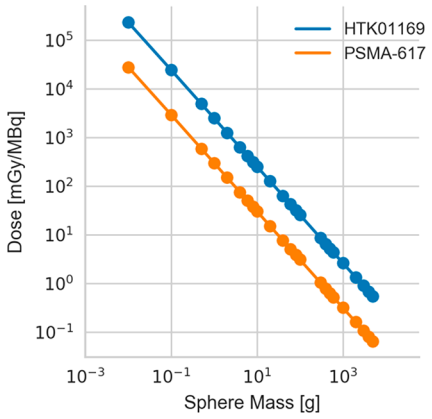

Figure 6. Radiation doses (mGy/MBq) of ^{177}Lu-PSMA-617 and ^{177}Lu-HTK01169 to LNCaP tumors calculated using the OLINDA software. These data were obtained with various tumor masses but assuming the same tumor uptake (%ID) and residence time for ^{177}Lu-PSMA-617 and ^{177}Lu-HTK01169.

treated with ^{177}Lu-HTK01169 (Groups C−F in Table 1 and Figures S7−S10) depended on the injected radioactivity, with higher radioactivity leading to more effective and prolonged tumor growth inhibition. The median survivals for the groups of mice treated with 18.5, 9.3, 4.6, and 2.3 MBq of ^{177}Lu-HTK01169 were >120, 103, 61, and 28 days, respectively. No weight loss was observed for all mice regardless of their treatment (Figures S4−S10), and all mice treated with 18.5 MBq of ^{177}Lu-HTK01169 (Group C in Table 1) survived until the end of the study (Day 120).

DISCUSSION

The use of small-molecule albumin binders to extend the circulation time of pharmaceuticals and maximize their tumor uptake has become an attractive strategy for the design of endoradiotherapeutic agents. The pioneering work was conducted mainly by ETH Zurich scientists using a D-Lys acylated at the ε-amino group with a 4-(*p*-iodophenyl)butyric acid as the albumin-binding motif.[22] Previous studies focused on applying this strategy to the design of folate-receptor-targeted radiopharmaceuticals.[23] As folate-receptor-α and proton-coupled folate transporter are highly expressed in renal proximal tubules, radiolabeled folate derivatives generally result in very high and sustained kidney uptake.[23] Radiolabeled folate derivatives with a built-in albumin binder were reported to significantly extend blood retention time, increase tumor uptake, and improve tumor-to-kidney uptake ratios.[23]

Recently, attempts were also made to use this strategy for the design of PSMA-targeted endoradiotherapeutic agents with the same or modified albumin-binding motifs (Figure 1).[24−28] Among the reported albumin-conjugated PSMA-targeted agents, ^{177}Lu-PSMA-ALB-02, ^{177}Lu-PSMA-ALB-056, and ^{177}Lu-RPS-063 were shown to deliver around 1.8-, 2.3-, and 3.8-fold higher radiation doses than ^{177}Lu-PSMA-617 to PSMA-expressing tumors.[26−28] In addition, ^{177}Lu-PSMA-ALB-056 was further evaluated in an endoradiotherapy study in mice bearing PSMA-expressing PC-3 PIP tumors.[27] The mice treated with ^{177}Lu-PSMA-617 or ^{177}Lu-PSMA-ALB-056 showed extended median survival when compared with the mice in the control group treated with saline. Most importantly, using only 2 MBq of ^{177}Lu-PSMA-ALB-056 was able to produce a slightly better median survival when compared to that from using 5 MBq of ^{177}Lu-PSMA-617 (36 vs 32 days).

Chen's group reported the synthesis and evaluation of ^{90}Y-DOTA-EB-MCG (Figure 1), a PSMA-targeted radiotherapeutic agent conjugated with a truncated Evans blue as the albumin-binding motif.[29] Compared with ^{90}Y-DOTA-MCG, which does not have the albumin-binding motif, ^{90}Y-DOTA-EB-MCG delivered a 4.4-fold higher radiation dose to PC-3 PIP tumor xenografts. The endoradiotherapy study also showed that PC-3 PIP tumor-bearing mice injected with 3.7 MBq of ^{90}Y-DOTA-EB-MCG had extended survival time compared to the mice injected with 7.4 MBq of ^{90}Y-DOTA-MCG. Recently, the same truncated Evans blue was conjugated to PSMA-617 to obtain ^{90}Y-EB-PSMA-617 and ^{177}Lu-EB-PSMA-617 with extended blood residence time and enhanced tumor uptake.[30] The endoradiotherapy study showed that a single dose of ^{90}Y-EB-PSMA-617 (1.85 MBq) or ^{177}Lu-EB-PSMA-617 (3.7 MBq) was sufficient to eradicate established PC-3 PIP tumors in mice.[30]

In this study, we exploited the conjugation of a novel albumin binder to further improve the tumor uptake of ^{177}Lu-PSMA-617, the most studied PSMA-targeted endoradiotherapeutic agent. Unlike the truncated Evans blue that has limited options for modification, the 4-(*p*-iodophenyl)butyric acid-containing motif is more flexible for modifications to optimize the blood retention time. For example, as shown in Figure 1, PSMA-ALB-56 contains a 4-methyl rather than a 4-iodo group in the albumin-binding motif, whereas RPS-027 has a shorter methylene rather than a propylene group between the 4-iodophenyl and the carboxylate groups. The most common albumin-binding motif reported in the literature consisted of a D-Lys that is acylated by 4-(*p*-iodophenyl)butyric acid at the ε-amino group.[22,23] Since the α-carboxylic group of D-Lys is part of the albumin-binding motif, it cannot be used for conjugation to the peptide via solid-phase synthesis.[31] To address this problem, a novel albumin binder was designed. As shown in the structure of Lu-HTK01169 (Figure 1), we replaced D-Lys with Glu. The carboxylic group at the Glu side chain can be used for binding to albumin, and the α-carboxylic group is used for conjugation to the peptide via solid-phase synthesis. It is well established that modification of the linker between

Table 1. Data of the Radiotherapy Study

		injected radioactivity (MBq)		tumor volume (mm^3)	
group	treatment (n = 8)	theoretical	measured (mean ± SD)	day 0 (mean ± SD)	median survival (day)
A	saline			440 ± 59	14
B	^{177}Lu-PSMA-617	18.5	18.9 ± 0.9	589 ± 93	58
C	^{177}Lu-HTK01169	18.5	18.8 ± 1.6	531 ± 239	>120
D	^{177}Lu-HTK01169	9.3	9.7 ± 0.3	640 ± 221	103
E	^{177}Lu-HTK01169	4.6	4.5 ± 0.2	586 ± 117	61
F	^{177}Lu-HTK01169	2.3	2.3 ± 0.1	545 ± 124	28

DOI: 10.1021/acs.molpharmaceut.8b00720
Mol. Pharmaceutics 2018, 15, 5183−5191

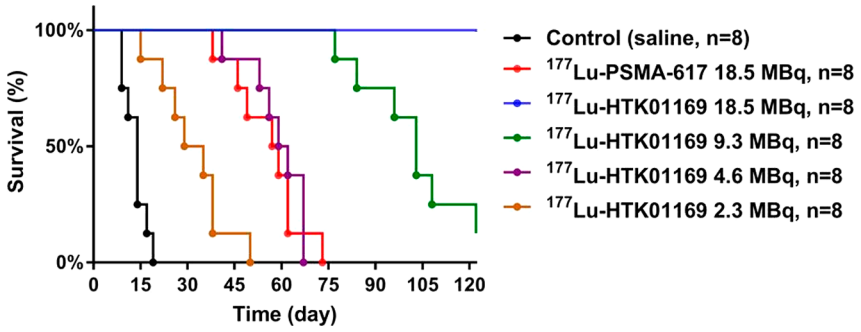

Figure 7. Overall survival for LNCaP tumor-bearing mice (n = 8 per group) injected with saline (the control group), ^{177}Lu-PSMA-617 (18.5 MBq), or ^{177}Lu-HTK01169 (2.3−18.5 MBq).

the DOTA chelator and PSMA-targeting Lys−urea−Glu is tolerated.[17] In fact, we observed a 6-fold improvement in PSMA binding for Lu-HTK01169 compared to Lu-PSMA-617 (K_i values: 0.04 ± 0.01 vs 0.24 ± 0.06 nM) possibly due to the introduction of the highly lipophilic 4-(*p*-iodophenyl)butyryl group.

The ability of ^{177}Lu-HTK01169 to bind albumin was assessed by the plasma-protein-binding assay. In contrast to the ∼17% of free ^{177}Lu-PSMA-617, only <1% of ^{177}Lu-HTK01169 was observed under the same conditions, demonstrating the capability of the albumin binder modified derivative to interact with plasma proteins. Part, but not all, of the observed difference may be explained by higher nonspecific interactions of ^{177}Lu-HTK01169 with the centrifugal filter.

The addition of an albumin binder to extend the blood retention time and maximize tumor uptake were confirmed by SPECT/CT and biodistribution studies. ^{177}Lu-HTK01169 not only showed improved peaked tumor uptake (^{177}Lu-HTK01169:55.9 ± 12.5%ID/g; ^{177}Lu-PSMA-617:15.1 ± 5.58%ID/g), but most importantly, the uptake was sustained rather than decreasing over time like ^{177}Lu-PSMA-617. This could be due to, in part, the improved PSMA binding of Lu-HTK01169 over Lu-PSMA-617. Compared with ^{177}Lu-PSMA-617, improved uptake combined with longer residence time provided an 8.3-fold higher radiation dose of ^{177}Lu-PSMA-617 to LNCaP tumor xenografts. Such a design strategy may be even more significant for radioisotopes with a longer half-life such as the α-emitter ^{225}Ac ($t_{1/2}$: ^{225}Ac, 9.95 d; ^{177}Lu, 6.65 d). Currently, the clinically used ^{225}Ac is extracted from ^{229}Th and is in limited supply.[32,33] Switching from ^{225}Ac-PSMA-617 to ^{225}Ac-HTK01169 may significantly increase the number of patients who can be treated with ^{225}Ac-labeled PSMA-targeting radioligands.

We observed a quick reduction in size of LNCaP tumor xenografts over time with the injection of ∼37 MBq of either ^{177}Lu-PSMA-617 or ^{177}Lu-HTK01169 (Figure 3). The ∼37 MBq injected radioactivity used for the acquisition of high-resolution SPECT images could have exceeded the dose of ^{177}Lu-HTK01169 needed to treat LNCaP tumors. Therefore, for the endoradiotherapy study, we compared the median survivals of mice treated with 18.5 MBq of ^{177}Lu-PSMA-617 or ^{177}Lu-HTK01169 as well as with only one-half (9.3 MBq), one-quarter (4.6 MBq), or one-eighth (2.3 MBq) of a dose of ^{177}Lu-HTK01169. The one-eighth dose (2.3 MBq) of ^{177}Lu-HTK01169 did not produce a similar median survival when compared to that of ^{177}Lu-PSMA-617 (18.5 MBq, Table 1) as predicted from the dosimetry data. However, we did observe that the median survival of mice treated with a one-quarter dose (4.5 MBq) of ^{177}Lu-HTK01169 was slightly better than that of mice treated with 18.5 MBq of ^{177}Lu-PSMA-617 (61 vs 58 days, Table 1).

There are two main differences between our study and the previous studies reported by the research groups of Müller (^{177}Lu-PSMA-ALB-056) and Chen (^{90}Y-DOTA-EB-MCG, ^{90}Y-EB-PSMA-617, and ^{177}Lu-EB-PSMA-617).[27,29,30] For the tumor model, we used LNCaP, an unmodified endogenous prostate cancer cell line. The previously reported studies used PC-3 PIP, a transduced cell line with a much higher PSMA expression level than LNCaP cells.[27,29,30] Consequently, most of the treatment doses of ^{177}Lu-PSMA-ALB-056 (2 and 5 MBq), ^{90}Y-DOTA-EB-MCG (3.7 and 7.4 MBq), ^{90}Y-EB-PSMA-617 (1.85−7.4 MBq), and ^{177}Lu-EB-PSMA-617 (3.7−18.5 MBq) in the previous reports were lower than those used in our study (2.3−18.5 MBq). The second difference is the size of tumors. Unlike the ∼100−150 mm^3 average tumor size in the previous reports,[27,29,30] the range of tumor sizes when treatment began with ^{177}Lu-PSMA-617 or ^{177}Lu-HTK01169 in this study was 531−640 mm^3. The larger tumors in our study likely conferred a higher degree of resistance to the treatment and subsequently required a higher radiation dose to achieve the similar growth inhibition.

One potential concern of using ^{177}Lu-HTK01169 to treat prostate cancer patients is its high dose delivered to kidney (see Supplemental Tables 3 and 4). The 8.3-fold higher radiation dose to tumors is accompanied by a 17.1-fold higher radiation dose to kidney when comparing ^{177}Lu-HTK01169 and ^{177}Lu-PSMA-617. However, it should be noted that the predicted high human kidney dose of ^{177}Lu-HTK01169 extrapolated from mouse kidney uptake data might be overestimated. Unlike human kidneys that have only moderate PSMA expression, PSMA is highly expressed in mouse kidneys.[34] In addition, other developments such as the use of 2-(phosphonomethyl)-pentanedioic acid (PMPA) and mannitol to reduce kidney uptake of PSMA-targeted radiopharmaceuticals have shown promising results in preclinical studies.[35,36] It would be interesting to attempt these strategies with ^{177}Lu-HTK01169 in future studies.

Another potential concern is the higher dose of ^{177}Lu-HTK01169 to bone marrow caused by its extended blood retention time. This will be of less concern if one were to use ^{225}Ac as the therapeutic radioisotope. The short-range (50−100 μm) of ^{225}Ac α-particles may result in less damage to bone marrow. Recently, ^{225}Ac-PSMA-617 was used to cure a patient with diffuse red marrow infiltration of metastatic castration-resistant prostate cancer without causing observable hematologic toxicity.[15] Another strategy to reduce the radiation dose to bone marrow is by selecting a less potent albumin binder to

DOI: 10.1021/acs.molpharmaceut.8b00720
Mol. Pharmaceutics 2018, 15, 5183−5191

reduce blood retention time without compromising overall tumor uptake. This could be achieved by optimization of the substitution (iodo vs bromo vs methyl) on the *para* position of the phenyl group (Figure 1)[22,27] and/or the selection of linker (propylene vs ethylene vs methylene) between the phenyl group and the amide bond.[25]

One limitation of our study is that we did not collect salivary glands, and therefore, the radiation doses to salivary glands from ^{177}Lu-PSMA-617 and ^{177}Lu-HTK01169 cannot be accurately estimated and compared. Salivary gland uptake is a main concern for using PSMA-targeted radiotherapeutic agents to treat metastatic castration-resistant prostate cancer[37] and is also the dose-limiting factor for using ^{225}Ac-PSMA-617.[38] However, it has been reported previously by Benešova et al. that ^{177}Lu-PSMA-617 and its albumin-binder-conjugated analogues showed no uptake in mouse salivary glands.[26]

Finally, in the first prospective study with ^{177}Lu-PSMA-617, renal and marrow toxicities were uncommon.[14] The latter may occur mainly in patients with extensive bone marrow infiltration. The relationship between enhanced efficacy at the expense of toxicity will require further investigation with this family of compounds.

CONCLUSIONS

Compared to ^{177}Lu-PSMA-617, the albumin-binder-conjugated ^{177}Lu-HTK01169 delivered 3.7-fold higher peak uptake and 8.3-fold higher overall radiation dose to LNCaP tumor xenografts. The endoradiotherapy study in LNCaP tumor-bearing mice also showed that only a quarter of the administered activity of ^{177}Lu-PSMA-617 is needed for ^{177}Lu-HTK01169 to achieve similar treatment efficacy. When translated to the clinic, HTK01169 radiolabeled with ^{177}Lu or ^{225}Ac could potentially also produce similar or improved radiotherapeutic efficacy with only a fraction of administered activity of ^{177}Lu-PSMA-617 or ^{225}Ac-PSMA-617. Whether those benefits will be hindered by normal organ toxicity will require further investigation. The newly introduced albumin binder in HTK01169 can be constructed directly on solid-phase along peptide elongation. Based on promising data obtained from ^{177}Lu-HTK01169, this new albumin-binding motif could potentially be applied to other (radio)peptides to extend their blood retention times and maximize therapeutic efficacy.

ASSOCIATED CONTENT

Supporting Information

The Supporting Information is available free of charge on the ACS Publications website at DOI: 10.1021/acs.molpharmaceut.8b00720.

Radiation dosimetry calculation procedures and additional data of ^{177}Lu-PSMA-617 and ^{177}Lu-HTK01169 (biodistribution, radiation dosimetry, semipreparative and analytical HPLC chromatograms, and changes of tumor volume and mouse body weight during the radiotherapy study) (PDF)

AUTHOR INFORMATION

Corresponding Authors

*Mailing Address: Kuo-Shyan Lin, Department of Molecular Oncology, BC Cancer, 675 West 10th Avenue, Rm 4-123, Vancouver, BC V5Z 1L3, Canada; Phone: 604-675-8208; Fax: 604-675-8218; E-mail: klin@bccrc.ca (K.-S.L.)

*Mailing Address: François Bénard, Department of Molecular Oncology, BC Cancer, 675 West 10th Avenue, Rm 14-111, Vancouver, BC V5Z 1L3, Canada; Phone: 604-675-8206; Fax: 604-675-8218; E-mail: fbenard@bccrc.ca (F.B.)

ORCID

Chengcheng Zhang: 0000-0001-5786-4748
Nadine Colpo: 0000-0001-9253-6539
Kuo-Shyan Lin: 0000-0002-0739-0780

Notes

The authors declare no competing financial interest.

ACKNOWLEDGMENTS

This work was supported by the Canadian Institutes of Health Research (FDN-148465), the Medical Imaging Clinical Trials Network of Canada, the Prostate Cancer Foundation BC, and the BC Leading Edge Endowment Fund.

REFERENCES

(1) Carter, R. E.; Feldman, A. R.; Coyle, J. T. Prostate-specific membrane antigen is a hydrolase with substrate and pharmacologic characteristics of a neuropeptidase. *Proc. Natl. Acad. Sci. U. S. A.* **1996**, *93*, 749−753.

(2) Silver, D. A.; Pellicer, I.; Fair, W. R.; Heston, W. D.; Cordon-Cardo, C. Prostate-specific membrane antigen expression in normal and malignant human tissues. *Clin. Cancer Res.* **1997**, *3*, 81−85.

(3) Sokoloff, R. L.; Norton, K. C.; Gasior, C. L.; Marker, K. M.; Grauer, L. S. A dual-monoclonal sandwich assay for prostate-specific membrane antigen: levels in tissues, seminal fluid and urine. *Prostate* **2000**, *43*, 150−157.

(4) Bander, N. H.; Milowsky, M. I.; Nanus, D. M.; Kostakoglu, L.; Vallabhajosula, S.; Goldsmith, S. J. Phase I trial of ^{177}lutetium-labeled J591, a monoclonal antibody to prostate-specific membrane antigen, in patients with androgen-independent prostate cancer. *J. Clin. Oncol.* **2005**, *23*, 4591−4601.

(5) Afshar-Oromieh, A.; Haberkorn, U.; Zechmann, C.; Armor, T.; Mier, W.; Spohn, F.; Debus, N.; Holland-Letz, T.; Babich, J.; Kratochwil, C. Repeated PSMA-targeting radioligand therapy of metastatic prostate cancer with ^{131}I-MIP-1095. *Eur. J. Nucl. Med. Mol. Imaging* **2017**, *44*, 950−959.

(6) Heck, M. M.; Retz, M.; D'Alessandria, C.; Rauscher, I.; Scheidhauer, K.; Maurer, T.; Storz, E.; Janssen, F.; Schottelius, M.; Wester, H. J.; Gschwend, J. E.; Schwaiger, M.; Tauber, R.; Eiber, M. Systemic radioligand therapy with ^{177}Lu labeled prostate specific membrane antigen ligand for imaging and therapy in patients with metastatic castration resistant prostate cancer. *J. Urol.* **2016**, *196*, 382−391.

(7) Kratochwil, C.; Giesel, F. L.; Stefanova, M.; Benešova, M.; Bronzel, M.; Afshar-Oromieh, A.; Mier, W.; Eder, M.; Kopka, K.; Haberkorn, U. PSMA-targeted radionuclide therapy of metastatic castration-resistant prostate cancer with ^{177}Lu-labeled PSMA-617. *J. Nucl. Med.* **2016**, *57*, 1170−1176.

(8) Rahbar, K.; Bode, A.; Weckesser, M.; Avramovic, N.; Claesener, M.; Stegger, L.; Bogemann, M. Radioligand therapy with ^{177}Lu-PSMA-617 as a novel therapeutic option in patients with metastatic castration resistant prostate cancer. *Clin. Nucl. Med.* **2016**, *41*, 522−528.

(9) Fendler, W. P.; Reinhardt, S.; Ilhan, H.; Delker, A.; Boning, G.; Gildehaus, F. J.; Stief, C.; Bartenstein, P.; Gratzke, C.; Lehner, S.; Rominger, A. Preliminary experience with dosimetry, response and patient reported outcome after ^{177}Lu-PSMA-617 therapy for metastatic castration-resistant prostate cancer. *Oncotarget* **2017**, *8*, 3581−3590.

(10) Rahbar, K.; Ahmadzadehfar, H.; Kratochwil, C.; Haberkorn, U.; Schafers, M.; Essler, M.; Baum, R. P.; Kulkarni, H. R.; Schmidt, M.; Drzezga, A.; Bartenstein, P.; Pfestroff, A.; Luster, M.; Lutzen, U.; Marx, M.; Prasad, V.; Brenner, W.; Heinzel, A.; Mottaghy, F. M.; Ruf,

DOI: 10.1021/acs.molpharmaceut.8b00720
Mol. Pharmaceutics 2018, 15, 5183−5191

J.; Meyer, P. T.; Heuschkel, M.; Eveslage, M.; Bogemann, M.; Fendler, W. P.; Krause, B. J. German multicenter study investigating ^{177}Lu-PSMA-617 radioligand therapy in advanced prostate cancer patients. *J. Nucl. Med.* **2017**, *58*, 85−90.
(11) Ahmadzadehfar, H.; Wegen, S.; Yordanova, A.; Fimmers, R.; Kurpig, S.; Eppard, E.; Wei, X.; Schlenkhoff, C.; Hauser, S.; Essler, M. Overall survival and response pattern of castration-resistant metastatic prostate cancer to multiple cycles of radioligand therapy using [^{177}Lu]Lu-PSMA-617. *Eur. J. Nucl. Med. Mol. Imaging* **2017**, *44*, 1448−1454.
(12) Brauer, A.; Grubert, L. S.; Roll, W.; Schrader, A. J.; Schafers, M.; Bogemann, M.; Rahbar, K. ^{177}Lu-PSMA-617 radioligand therapy and outcome in patients with metastasized castration-resistant prostate cancer. *Eur. J. Nucl. Med. Mol. Imaging* **2017**, *44*, 1663−1670.
(13) Yadav, M. P.; Ballal, S.; Tripathi, M.; Damle, N. A.; Sahoo, R. K.; Seth, A.; Bal, C. ^{177}Lu-DKFZ-PSMA-617 therapy in metastatic castration resistant prostate cancer: safety, efficacy, and quality of life assessment. *Eur. J. Nucl. Med. Mol. Imaging* **2017**, *44*, 81−91.
(14) Hofman, M. S.; Violet, J.; Hicks, R. J.; Ferdinandus, J.; Thang, S. P.; Akhurst, T.; Iravani, A.; Kong, G.; Kumar, A. R.; Murphy, D. G.; Eu, P.; Jackson, P.; Scalzo, M.; Williams, S. G.; Sandhu, S. [^{177}Lu]-PSMA-617 radionuclide treatment in patients with metastatic castration-resistant prostate cancer (LuPSMA trial): a single-centre, single-arm, phase 2 study. *Lancet Oncol.* **2018**, *19*, 825−833.
(15) Kratochwil, C.; Bruchertseifer, F.; Giesel, F. L.; Weis, M.; Verburg, F. A.; Mottaghy, F.; Kopka, K.; Apostolidis, C.; Haberkorn, U.; Morgenstern, A. ^{225}Ac-PSMA-617 for PSMA-targeted α-radiation therapy of metastatic castration-resistant prostate cancer. *J. Nucl. Med.* **2016**, *57*, 1941−1944.
(16) Benešova, M.; Schafer, M.; Bauder-Wust, U.; Afshar-Oromieh, A.; Kratochwil, C.; Mier, W.; Haberkorn, U.; Kopka, K.; Eder, M. Preclinical evaluation of a tailor-made DOTA-conjugated PSMA inhibitor with optimized linker moiety for imaging and endoradiotherapy of prostate cancer. *J. Nucl. Med.* **2015**, *56*, 914−920.
(17) Benesova, M.; Bauder-Wust, U.; Schafer, M.; Klika, K. D.; Mier, W.; Haberkorn, U.; Kopka, K.; Eder, M. Linker modification strategies to control the prostate-specific membrane antigen (PSMA)-targeting and pharmacokinetic properties of DOTA-conjugated PSMA inhibitors. *J. Med. Chem.* **2016**, *59*, 1761−1775.
(18) Kuo, H. T.; Pan, J.; Zhang, Z.; Lau, J.; Merkens, H.; Zhang, C.; Colpo, N.; Lin, K. S.; Benard, F. Effects of linker modification on tumor-to-kidney contrast of ^{68}Ga-labeled PSMA-targeted imaging probes. *Mol. Pharmaceutics* **2018**, *15*, 3502.
(19) Meckel, M.; Kubicek, V.; Hermann, P.; Miederer, M.; Rosch, F. A DOTA based bisphosphonate with an albumin binding moiety for delayed body clearance for bone targeting. *Nucl. Med. Biol.* **2016**, *43*, 670−678.
(20) Harada, N.; Kimura, H.; Onoe, S.; Watanabe, H.; Matsuoka, D.; Arimitsu, K.; Ono, M.; Saji, H. Synthesis and biological evaluation of novel ^{18}F-labeled probes targeting prostate-specific membrane antigen for positron emission tomography of prostate cancer. *J. Nucl. Med.* **2016**, *57*, 1978−1984.
(21) Chatalic, K. L. S.; Heskamp, S.; Konijnenberg, M.; Molkenboer-Kuenen, J. D. M.; Franssen, G. M.; Clahsen-van Groningen, M. C.; Schottelius, M.; Wester, H. J.; van Weerden, W. M.; Boerman, O. C.; de Jong, M. Towards personalized treatment of prostate cancer: PSMA I&T, a promising prostate-specific membrane antigen-targeted theranostic agent. *Theranostics* **2016**, *6*, 849−861.
(22) Dumelin, C. E.; Trussel, S.; Buller, F.; Trachsel, E.; Bootz, F.; Zhang, Y.; Mannocci, L.; Beck, S. C.; Drumea-Mirancea, M.; Seeliger, M. W.; Baltes, C.; Muggler, T.; Kranz, F.; Rudin, M.; Melkko, S.; Scheuermann, J.; Neri, D. A portable albumin binder from a DNA-encoded chemical library. *Angew. Chem., Int. Ed.* **2008**, *47*, 3196−3201.
(23) Muller, C.; Struthers, H.; Winiger, C.; Zhernosekov, K.; Schibli, R. DOTA conjugate with an albumin-binding entity enables the first folic acid-targeted ^{177}Lu-radionuclide tumor therapy in mice. *J. Nucl. Med.* **2013**, *54*, 124−131.
(24) Choy, C. J.; Ling, X.; Geruntho, J. J.; Beyer, S. K.; Latoche, J. D.; Langton-Webster, B.; Anderson, C. J.; Berkman, C. E. ^{177}Lu-Labeled phosphoramidate-based PSMA inhibitors: The effect of an albumin binder on biodistribution and therapeutic efficacy in prostate tumor-bearing mice. *Theranostics* **2017**, *7*, 1928−1939.
(25) Kelly, J. M.; Amor-Coarasa, A.; Nikolopoulou, A.; Wustemann, T.; Barelli, P.; Kim, D.; Williams, C.; Zheng, X.; Bi, C.; Hu, B.; Warren, J. D.; Hage, D. S.; DiMagno, S. G.; Babich, J. W. Dual-target binding ligands with modulated pharmacokinetics for endoradiotherapy of prostate cancer. *J. Nucl. Med.* **2017**, *58*, 1442−1449.
(26) Benesova, M.; Umbricht, C. A.; Schibli, R.; Müller, C. Albumin-binding PSMA ligands: optimization of the tissue distribution profile. *Mol. Pharmaceutics* **2018**, *15*, 934−946.
(27) Umbricht, C. A.; Benesova, M.; Schibli, R.; Müller, C. Preclinical development of novel PSMA-targeting radioligands: Modulation of albumin-binding properties to improve prostate cancer therapy. *Mol. Pharmaceutics* **2018**, *15*, 2297−2306.
(28) Kelly, J.; Amor-Coarasa, A.; Ponnala, S.; Nikolopoulou, A.; Williams, C.; Schlyer, D.; Zhao, Y.; Kim, D.; Babich, J. W. Trifunctional PSMA-targeting constructs for prostate cancer with unprecedented localization to LNCaP tumors. *Eur. J. Nucl. Med. Mol. Imaging* **2018**, *45*, 1841.
(29) Wang, Z.; Jacobson, O.; Tian, R.; Mease, R. C.; Kiesewetter, D. O.; Niu, G.; Pomper, M. G.; Chen, X. Radioligand therapy of prostate cancer with a long-lasting prostate-specific membrane antigen targeting agent ^{90}Y-DOTA-EB-MCG. *Bioconjugate Chem.* **2018**, *29*, 2309−2315.
(30) Wang, Z.; Tian, R.; Niu, G.; Ma, Y.; Lang, L.; Szajek, L. P.; Kiesewetter, D. O.; Jacobson, O.; Chen, X. Single low-dose injection of Evans blue modified PSMA-617 radioligand therapy eliminates prostate-specific membrane antigen positive tumors. *Bioconjugate Chem.* **2018**, *29*, 3213.
(31) Liu, Z.; Chen, X. Simple Bioconjugate chemistry serves great clinical advances: albumin as a versatile platform for diagnosis and precision therapy. *Chem. Soc. Rev.* **2016**, *45*, 1432−1456.
(32) Apostolidis, C.; Molinet, R.; Rasmussen, G.; Morgenstern, A. Production of Ac-225 from Th-229 for targeted α therapy. *Anal. Chem.* **2005**, *77*, 6288−6291.
(33) Walsh, K. M. Brookhaven National Laboratory: Radioisotopes for medical imaging and disease treatment. *J. Nucl. Med.* **2017**, *58*, 11N−12N.
(34) Bacich, D. J.; Pinto, J. T.; Tong, W. P.; Heston, W. D. W. Cloning, expression, genomic localization, and enzymatic activities of the mouse homolog of prostate-specific membrane antigen/NAALADase/folate hydrolase. *Mamm. Genome* **2001**, *12*, 117−123.
(35) Kratochwil, C.; Giesel, F. L.; Leotta, K.; Eder, M.; Hoppe-Tich, T.; Youssoufian, H.; Kopka, K.; Babich, J. W.; Haberkorn, U. PMPA for nephroprotection in PSMA-targeted radionuclide therapy of prostate cancer. *J. Nucl. Med.* **2015**, *56*, 293−298.
(36) Matteucci, F.; Mezzenga, E.; Caroli, P.; Di Iorio, V.; Sarnelli, A.; Celli, M.; Fantini, L.; Moretti, A.; Galassi, R.; De Giorgi, U.; Paganelli, G. Reduction of ^{68}Ga-PSMA renal uptake with mannitol infusion: preliminary results. *Eur. J. Nucl. Med. Mol. Imaging* **2017**, *44*, 2189−2194.
(37) Langbein, T.; Chausse, G.; Baum, R. P. Salivary gland toxicity of PSMA radioligand therapy: relevance and preventive strategies. *J. Nucl. Med.* **2018**, *59*, 1172.
(38) Kratochwil, C.; Bruchertseifer, F.; Rathke, H.; Bronzel, M.; Apostolidis, C.; Weichert, W.; Haberkorn, U.; Giesel, F. L.; Morgenstern, A. Targeted α-therapy of metastatic castration-resistant prostate cancer with ^{225}Ac-PSMA-617: dosimetry estimate and empiric dose finding. *J. Nucl. Med.* **2017**, *58*, 1624−1631.

DOI: 10.1021/acs.molpharmaceut.8b00720
Mol. Pharmaceutics 2018, 15, 5183−5191